MOLECULAR AND CELLULAR BIOLOGY, Mar. 2010, p. 1457–1466 Vol. 30, No. 6
0270-7306/10/$12.00 doi:10.1128/MCB.01321-09

Yeast Exonuclease 5 Is Essential for Mitochondrial Genome Maintenance[▽]

Peter M. Burgers,* Carrie M. Stith, Bonita L. Yoder, and Justin L. Sparks

Department of Biochemistry and Molecular Biophysics, Washington University School of Medicine, St. Louis, Missouri 63110

Received 30 September 2009/Returned for modification 9 November 2009/Accepted 5 January 2010

Yeast exonuclease 5 is encoded by the YBR163w (*DEM1*) gene, and this gene has been renamed *EXO5*. It is distantly related to the *Escherichia coli* RecB exonuclease class. Exo5 is localized to the mitochondria, and *EXO5* deletions or nuclease-defective *EXO5* mutants invariably yield petites, amplifying either the *ori3* or *ori5* region of the mitochondrial genome. These petites remain unstable and undergo continuous rearrangement. The mitochondrial phenotype of *exo5*Δ strains suggests an essential role for the enzyme in DNA replication and recombination. No nuclear phenotype associated with *EXO5* deletions has been detected. Exo5 is a monomeric 5′ exonuclease that releases dinucleotides as products. It is specific for single-stranded DNA and does not hydrolyze RNA. However, Exo5 has the capacity to slide across 5′ double-stranded DNA or 5′ RNA sequences and resumes cutting two nucleotides downstream of the double-stranded-to-single-stranded junction or RNA-to-DNA junction, respectively.

Endonucleases and exonucleases are intimately involved in all aspects of DNA metabolism in the cell. In mitochondria, several constitutive nucleases have been identified that contribute to the proper maintenance of the mitochondrial genome through replication and recombination pathways. In addition, nucleases can localize to mitochondria in response to DNA stress in order to mediate appropriate DNA repair. Among the constitutive mitochondrial nucleases in *Saccharomyces cerevisiae* are the Nuc1 nuclease that contributes to DNA recombination efficiency and functions in apoptosis (4, 38) and the Cce1 endonuclease that resolves recombination intermediates (29). The Din7 endonuclease is a mitochondrially located 5′ flap endonuclease related to FEN1 (20). While deletion of the gene for either of these enzymes produced marginal mitochondrial phenotypes, more severe phenotypes were observed when combined deletions of these nuclease genes were studied or when they were combined with deletions of other genes involved in DNA recombination or repair, such as *MHR1* or *MSH1* (20, 22, 27). Recently, human Dna2 was shown to localize to both the nuclear and mitochondrial compartments and to participate in mitochondrial DNA replication and base excision repair (11, 39). Its function in yeast mitochondrial DNA maintenance has not been studied in detail. Finally, the 5′ flap endonuclease FEN1, which normally functions in primer RNA degradation during Okazaki fragment maturation in the nucleus, also localizes to the mitochondrion in response to DNA damage, participating in long-patch base excision repair (19, 23).

Since mitochondrial function is not essential to yeast survival, dysfunction caused by mutations of the mitochondrial genome can be readily detected as a loss of respiration function, which is scored as the inability to grow on nonfermentable carbon sources. A defect in the mitochondrial DNA polymerase γ *MIP1* results in complete loss of the mitochondrial DNA, and the mutant fails to grow on glycerol-containing media lacking glucose (14). Such cells are designated ρ^0. Genome maintenance defects can also result in the generation of petite mutants that still contain mitochondrial DNA. Generally, most of the mitochondrial genome has been deleted, and a small origin-containing region has been amplified (ρ^-). *S. cerevisiae* contains eight such origin regions that are highly similar in sequence and are distributed over the 86-kb mitochondrial genome (8, 9, 15). Petites that have amplified the *ori5* region have been studied more extensively (16, 22).

While the nucleases listed above participate in the proper maintenance of the mitochondrial genome through their replication and/or recombination functions, none appears to be essential for the integrity of the mitochondrial genome. One reasonable explanation for these observations is functional redundancy. Indeed, functional nuclease redundancy is quite common; it has been observed in the process of DNA degradation during mismatch repair in *Escherichia coli*, during Okazaki fragment maturation in yeast, and during the resection of double-stranded breaks in yeast (7, 25, 33). However, the possibility remains that an additional nuclease(s) is active in the mitochondrion. The present paper describes an essential mitochondrial exonuclease that is distantly related to the nuclease domain of RecB, a subunit of the bacterial RecBCD recombinase. This nuclease was discovered over 2 decades ago during a biochemical chromatographic survey of yeast exonucleases and was called exonuclease 5 (3). Initial studies with a partially purified enzyme preparation showed it to be a 5′ exonuclease specific for single-stranded DNA (ssDNA). Here we report the identification of the *EXO5* gene and describe comprehensive biochemical and genetic studies that show a critical role for *EXO5* in mitochondrial DNA maintenance, presumably through the processing of replication intermediates. Upon deletion of *EXO5* or inactivation of its nuclease activity, only ρ^- mutants could be recovered. *EXO5* has previously been characterized as *DEM1* (defects in morphology)

* Corresponding author. Mailing address: Department of Biochemistry and Molecular Biophysics, Washington University School of Medicine, St. Louis, MO 63110. Phone: (314) 362-3872. Fax: (314) 362-7183l. E-mail: burgers@biochem.wustl.edu.

▽ Published ahead of print on 19 January 2010.

because the deletion mutant shows defects in growth and in mitochondrial morphology (10, 12). No nuclear defect associated with an *EXO5* deletion has been detected.

MATERIALS AND METHODS

Plasmids and oligonucleotides. Plasmid pBL253 contains the YBR163w (*EXO5*) open reading frame (ORF) together with 249 nucleotides (nt) of 5′ untranslated sequence and 300 nt of 3′ untranslated sequence cloned into centromere vector yCp50 (*ARS1 CEN4 URA3*). Plasmid pBL256 contains the same *EXO5* region cloned into centromere vector yCplac22 (*ARS1 CEN4 TRP1*). Plasmids pBL256-270 and -320, with active-site mutations *exo5-D270A* and *exo5-D320A*, respectively, were made by site-directed mutagenesis, and the correct sequences were confirmed by sequencing of the entire gene. Plasmid pBL254 (bluescript 2μm ori *HIS3* M13 ori *GAL1-10* GST-*EXO5*) contains the *Schistosoma japonicum* glutathione *S*-transferase (GST) gene fused to the N terminus of the *EXO5* gene in vector pRS424-GALGST (5). The GST tag is separated from the *EXO5* gene by a recognition sequence for the human rhinoviral 3C protease (LEVLFQ/GP). After cleavage by the protease, the N-terminal sequence of the Exo5 polypeptide is extended with the GPEF sequence. Plasmids pBL254-270 and -320 have active-site mutations as in pBL256. Plasmids and sequences are available upon request.

Oligonucleotides were purchased from IDT (Coralville, IA) and purified by high-performance liquid chromatography or urea-polyacrylamide gel electrophoresis (PAGE): v31, GCCCATCAACGTTCCAGACC; c41, GGTCTGGAACGTTGATGGGC; cT41, TGGTCTGGAACGTTGATGGGC; c42, GGTCTGGAACGTTGATGGG; c43, GGTCTGGAACGTTGATGG; c44, GGTCTGGAACGTTGAT; c45, GGTCTGGAACGTTGATGGGCT$_{10}$; c48, GGTCTGGAACGTTGAT$_{10}$; c49, GAACGTTGATGGGC; c50, GGTCTGGAACGTTG; cT50, TGGTCTGGAACGTTG; v71, TCGAATTGGTCTTTTTTTTCC; vR73, UCGAAUUGGUCTTTTTTTTCC (RNA underlined); Bio-vR74, T^{Bio}CGAAUUGGUCTTTTTTTTCC; c72 GGAAAAAAAAGACCAATTCGA; v81, TTGCCGATGAACTTTTTTTTTTGATCGAGACCTT. The 5′ ^{32}P label was introduced on oligonucleotides v31, v71, vR73, Bio-vR74, and v81 with [γ-^{32}P]ATP and T4 polynucleotide kinase, while for the addition of a 3′ ^{32}P label, oligonucleotide v31 (containing an unlabeled 5′ phosphate) was incubated at a 10-fold molar excess over carrier-free [α-^{32}P]dATP with terminal deoxynucleotidyltransferase under the manufacturer's conditions, with an additional 150 mM KCl. The addition of salt limited processive addition by the enzyme, thereby ensuring mainly the addition of a single [^{32}P]dAMP residue. The labeled v oligonucleotides were hybridized with a twofold molar excess of the relevant c oligonucleotides. Labeled v81 was circularized by hybridization to equimolar oligonucleotide circ-81 (ATCGGCAAAAGGTCTC), which anneals to both 5′ and 3′ ends. After ligation with T4 ligase, the circular oligonucleotide was further purified on a urea–12% polyacrylamide gel.

Yeast strains. Deletions of *RAD27*, *EXO1*, *MUS81*, and *MRE11* were obtained as gene replacements with KanMX4 in BY4741 (*MAT***a** *his3-Δ1 leu2-Δ0 met15-Δ0 ura3-Δ0*). Strain PY207 (*MAT***a**/α *his3Δ1/his3Δ1 leu2Δ0/leu2Δ0 ura3Δ0/ura3Δ0 met15Δ0/+ lys2Δ/+ exo5Δ::HIS3/+* [*rho*$^+$]) was obtained by transformation of diploid BY4743 with *exo5Δ::HIS3*. PY209 (*MAT*α *his3-Δ1 leu2-Δ0 trp1-Δ0 ura3-Δ0 exo5Δ::HIS3* + pBL253 [*rho*$^+$]) was obtained from sporulation of PY207 after transformation with pBL253. Strain W303/mip1-01 (*MAT*α *ura3 his3 ade2 leu2 trp1 mip1-01::URA3* [*rho*^{0}]), from Francoise Foury, was made *exo5Δ::HIS3* by transformation to give PY215. This strain was mated with the BY4741 series of nuclease deletion strains to give [*rho*$^+$] heterozygous diploids. This series of diploids was sporulated, and appropriate haploids were selected, *mip1Δ* as Ura$^+$, *exo5Δ* as His$^+$, and *rad27Δ* (or other nuclease deletions) as G418 resistance. Genotypes were confirmed by diagnostic PCR analysis. These sets of strains were used in the analysis in Fig. 7.

Exo5 overproduction and purification. Overexpression was in *S. cerevisiae* strain PY116 (*MAT***a** *his3-11,15 ura3-52 trp1-Δ leu2-3,112 prb1-1122 prc1-407 pep4-3 nuc1Δ-LEU2*) transformed with pBL254. Growth, induction, and extract preparation were essentially as described elsewhere (5). Briefly, cells (60 g of packed cells resuspended in 12 ml of water) frozen previously in liquid nitrogen in the form of popcorn were blended in dry ice powder with 30 ml of buffer 3 × A (buffer A is 30 mM HEPES-NaOH [pH 7.8], 10% glycerol, 2 mM EDTA, 1 mM EGTA, 0.02% Nonidet P-40, 2 mM dithiothreitol [DTT], 10 mM sodium bisulfite, 10 μM pepstatin A, 10 μM leupeptin). All further operations were carried out at 0 to 4°C. After thawing of the lysate, 0.5 mM phenylmethylsulfonyl fluoride (from a 100 mM stock in ethanol) and 150 mM ammonium sulfate (from a 4 M stock) were stirred in, followed by 0.45% polymin P (from a 10% stock at pH 7.3). After being stirred for 15 min, the lysate was cleared at 40,000 × *g* for 30 min and the supernatant was precipitated with 0.31 g/ml solid ammonium sulfate. The precipitate was collected by centrifugation at 40,000 × *g* for 20 min and redissolved in ~50 ml of buffer A until the conductivity equaled that of buffer A$_{300}$ (the subscript denotes the NaCl concentration). Batch binding to 1 ml of glutathione-Sepharose 4B beads (GE Healthcare), equilibrated previously in buffer A$_{300}$, was done by gentle rotation in the cold room for 2 h. The beads were collected at 1,000 rpm in a swinging-bucket rotor, batch washed by resuspension and spinning with 2 × 20 ml of buffer A$_{300}$, transferred to a 10-ml column, and washed at 1 ml/min with 100 ml of buffer A$_{300}$. Bound chaperones, particularly Ssa1, were removed by washing with 50 ml of buffer A$_{300}$ containing 1 mM ATP and 5 mM Mg-acetate. After another wash with 10 ml of buffer A$_{150}$ to remove residual nucleotide and decrease the salt concentration, the beads were resuspended in 1 ml of buffer A$_{150}$ containing 20 mM glutathione (pH adjusted to 8.0). The capped column was incubated on ice for 10 min, and the eluant was collected. This procedure was repeated four times. Most of the protein eluted in fractions 1 to 4. These fractions were incubated overnight at 4°C with 30 U of rhinoviral 3C protease and, after dilution with buffer A$_0$ to equal buffer A$_{100}$, loaded onto a 1-ml heparin-Superose column. Protein was eluted with a linear gradient of buffer A$_{100}$ to buffer A$_{1000}$. Pure Exo5 eluted at 250 to 300 mM NaCl. Mutant forms of Exo5 were purified similarly through the GST-Sepharose step.

Enrichment of Exo5 from yeast extracts. Yeast single-ORF deletion derivatives of BY4741 were grown in 1 liter of YPD (2% peptone, 1% yeast extract, 2% glucose) to mid-log phase. The cells were harvested, and extracts were prepared by beating with glass beads, polymin P precipitation, and ammonium sulfate precipitation as described previously (3). Protein (1 mg) in buffer A$_{50}$ was gently agitated for 2 h with 200 μl of DEAE-Sephacel plus 200 μl of SP-Sepharose in a total volume of 1.5 ml. Under these buffer conditions, Exo5 does not bind to either matrix. Beads were spun down, and the supernatant was used for nuclease assays with 5′-^{32}P-labeled dT$_{12}$ substrate.

Exonuclease assays. The standard 20-μl assay mixture contained 20 mM HEPES-NaOH (pH 7.6), 20 μg/ml bovine serum albumin, 1 mM DTT, 5 mM Mg-acetate, 50 mM NaCl, 100 fmol of ^{32}P-labeled oligonucleotide substrate, and enzyme. Incubations were at 30°C for the indicated times. Variations from the standard assay are indicated in the legends to the figures. Reactions were stopped with 10 mM (final concentration) EDTA plus 0.2% SDS and analyzed by thin-layer chromatography (TLC) on polyethyleneimine-cellulose in 0.7 M LiCl or stopped with 10 mM (final concentration) EDTA plus 40% formamide and analyzed by 20% PAGE–7 M urea electrophoresis. After the TLC plate or gel was dried, it was subjected to PhosphorImager analysis.

PCR and Southern analysis. Total cellular chromosomal DNA preparations were made from 5-ml cultures grown overnight in selective media (17). These were subjected to 20 cycles of PCR in a 50-μl reaction mixture with 100 ng of chromosomal DNA and 50 pmol each of primers ori-in (GGGGGTCCCAATTATTATTTTC and TAGGGGGAGGGGGTGGGT), ori-out (primers complementary to ori-in: GAAAATAATAATTGGGACCCCC and ACCCACCCCCTCCCCCTA), *COX2* (GCATGTTATTTTCAGGATTCAGCAACACC and GAACCTTCAGCTTCAATAAAACCTAAAATTC), and *AI1* (GATACTCAATATGGAAAGCCGTATGATG and CGGACAATCCCGTATTTCTTAATTTTCC). Analysis was on a 2.5% metaphor agarose gel.

To label the *ori* sequences, the isolated *ori3* or *ori5* PCR fragment was reamplified by PCR with ori-in primers but with 10 μM [α-^{32}P]dATP and the other three deoxynucleoside triphosphates at 200 μM. The labeled *ori3* and *ori5* fragments were mixed and used as a probe of EcoRV-cut total cellular DNA. EcoRV cuts either origin near the end of the fragment (see Fig. 6).

RESULTS

Identification of the *S. cerevisiae EXO5* gene. Previously, we had partially purified Exo5 from yeast and established some of the properties of the enzyme (3). Specifically, we noted that the enzyme preferentially degraded ssDNA and produced dinucleotides as the main products of digestion. In order to further studies of this unique enzyme and gain an understanding of its physiological role in the cell, we first identified the gene for Exo5.

The enzyme was partially purified from yeast as described before, through four chromatographic steps (3). This preparation was further fractionated on a MonoQ column. Unfortunately, sodium dodecyl sulfate (SDS)-PAGE analysis still did

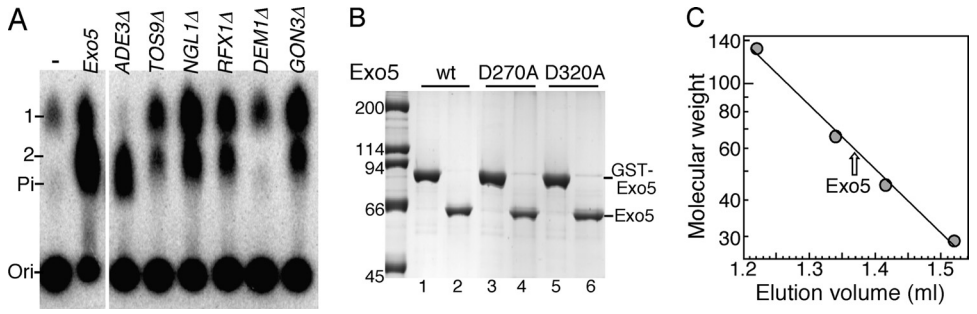

FIG. 1. Cloning of *EXO5* and overproduction of Exo5 nuclease. (A) Extracts from the indicated deletion mutants of strain BY4741 were subjected to partial purification. Standard assay mixtures contained 2 μl of the fraction that flowed through the mixed-bed ion exchanger (see Materials and Methods). Controls were no extract (−) or partially purified Exo5. Migration positions of phosphate (Pi) and mono- and dinucleotide (1 and 2, respectively) are indicated. (B) Overexpression and purification of Exo5. Lane 1, GST-Exo5 after glutathione column chromatography; lane 2, after cutting with 3C protease and heparin-Sepharose chromatography; lanes 3 and 4, the same for the Exo5-D270A mutant; lanes 5 and 6, the same for the Exo5-D320A mutant. Each lane contained ~2 μg of protein. wt, wild type. The values on the left are molecular sizes in kilodaltons. (C) Superose 12 gel filtration analysis of Exo5 in buffer A_{200}. Marker proteins are bovine serum albumin dimer and monomer, ovalbumin, and carbonic anhydrase.

not allow positive identification of a protein band that comigrated with exonuclease activity. Therefore, the fraction with the highest exonuclease activity and a neighboring fraction with much reduced enzyme activity but with a similar protein banding pattern were fractionated by SDS-PAGE and each of the two lanes was cut into 15 slices and subjected to liquid chromatography-tandem mass spectrometry analysis. Six yeast proteins (Ade3, Tos9, Ngl1, Rfx1, Dem1, and Gon3) that were present in greater abundance in the active lane than in the lane without activity were identified. In order to determine which one corresponded to Exo5, we obtained deletion strains for each one of these genes (none of the genes identified was essential for growth). Extracts were prepared, partially enriched for Exo5, and assayed for activity. Only the extract of the *dem1*Δ mutant strain lacked a dinucleotide-producing activity (Fig. 1A). This analysis suggests that the *DEM1* gene is required for Exo5 activity, and the simplest explanation is that it actually encodes Exo5.

An analysis of yeast protein databases revealed some information about YBR163w = *EXO5* = *DEM1*. The deletion mutant is respiration deficient and shows morphological defects of the mitochondrion, hence the original gene designation *DEM1* (*de*fects in *m*orphology) (12). Consistent with a mitochondrial function for *EXO5*/*DEM1*, the localization of the protein is mitochondrial (18). In support of this observed localization, the protein sequence contains a strong mitochondrial localization signal, using several prediction programs (MitoProt, Predotar), predicting cleavage at Ser26/Leu27 during mitochondrial import.

Overproduction and purification of Exo5 and Exo5 mutants. Exo5/Dem1 was overproduced in yeast from a multicopy plasmid with the *EXO5*/*DEM1* gene placed under the control of the galactose-inducible *GAL1-10* promoter. A cleavable GST tag was added to aid in purification (see Materials and Methods). Following glutathione affinity column chromatography, the GST tag was proteolytically cleaved and Exo5/Dem1 was further purified by heparin-agarose chromatography to more than 98% purity (Fig. 1B). Upon SDS-PAGE analysis, the protein migrated as a 64-kDa protein, in agreement with the size calculated from the ORF sequence (67 kDa). A gel filtration analysis showed that Exo5 migrated as a 58-kDa protein, indicating that Exo5 is a compact monomeric enzyme (Fig. 1C).

An analysis of the gel filtration fractions, using a 5′-labeled oligonucleotide as the substrate, showed potent exonuclease activity that comigrated with the protein peak (data not shown). In agreement with previous studies of the partially purified enzyme, dinucleotides were the main products of digestion (Fig. 2C and 3). Since these studies strongly suggest that the *DEM1* gene actually encodes exonuclease 5, we will from now on refer to this gene as *EXO5*.

We subjected *EXO5* to a PSI-BLAST analysis, followed by a protein threading analysis (http://toolkit.tuebingen.mpg.de/hhpred) (32). The PSI-BLAST analysis identified *EXO5* as the member of a poorly conserved protein family. Interestingly, the threading analysis that was carried out with the consensus sequence obtained from the PSI-BLAST analysis yielded bacterial RecB-type nucleases as top-scoring structural homologs of *EXO5* (Fig. 2A). Among the putative homologs in other model eukaryotic organisms are ORFC185.02 in *Schizosaccharomyces pombe* and C1orf176 in humans, both uncharacterized ORFs. While the conservation with *E. coli* RecB was restricted to just three small motifs in the C-terminal nuclease domain of RecB (Fig. 2A), the members of the eukaryotic Exo5 family showed conservation of a large number of small motifs over a core domain of ~250 amino acids (alignment not shown). Remarkably, a set of conserved cysteine residues in the C-terminal domain of the Exo5 members was conserved with the AddB nuclease domain of the *Bacillus subtilis* AddAB recombinase (36). In AddB, these cysteines coordinate an iron-sulfur cluster, suggesting that the Exo5 class may also possess this structural domain.

The first and second motifs conserved with the *E. coli* RecB nuclease are in two β strands that contain the two aspartates that chelate the divalent metal ion in the active site of the nuclease (31). The third conserved motif is in an α helix that overlies the active-site aspartates (Fig. 2B). Although the function of this α helix is not known, the proximity of the invariant glutamine and tyrosine to the active site is remarkable. Previous studies of RecB had shown that mutation of D1080, one of

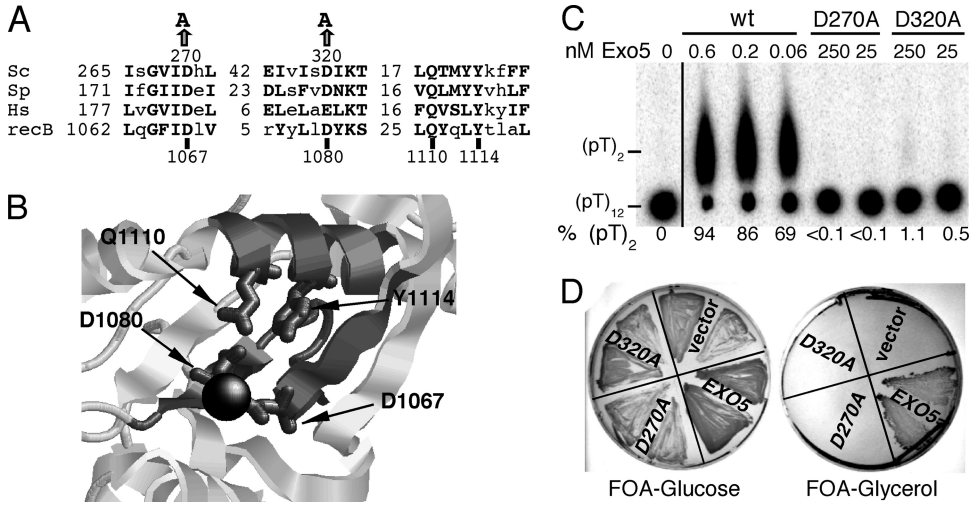

FIG. 2. Mutational analysis of *EXO5*. (A) Threading analysis of Exo5. Motifs conserved with *E. coli* RecB nuclease are shown. Sc, *S. cerevisiae*; Sp, *S. pombe*; Hs, *Homo sapiens*. (B) Active site of the RecB nuclease domain from the crystal structure of *E. coli* RecBCD (31). The active-site divalent metal ion (black) is coordinated by Asp1067 and Asp1080 (dark gray), which are part of the two gray beta strands, 1057 to 1072 and 1078 to 1082, respectively. The active site is closed off by the α helix at 1107 to 1125 (light gray) with the conserved Gln1110 and Tyr1114 residues (dark gray). (C) Standard nuclease assay mixtures contained the indicated concentrations of wild-type (wt) or mutant Exo5 for 10 min. Analysis was by TLC. (D) Strain PY209 (*exo5*Δ::*HIS3* but [*rho*$^+$] because it contains pBL253 [*EXO5 URA3*]) was transformed with the empty vector (vector) or pBL256 (*EXO5*), pBL256-270 (*exo5-D270A*), or pBL256-320 (*exo5-D320A*). Transformants were streaked onto FOA plates to select for loss of plasmid pBL253, with either glucose or glycerol as the carbon source. Plates were photographed after 2 days (glucose plates) or 4 days (glycerol plates) of growth at 30°C.

the aspartates that ligate the divalent metal ion, abolishes the exonuclease activity of RecB (37). Therefore, we mutated either putative active-site residue Asp270 or Asp320 to alanine, overproduced and purified the mutant proteins analogously to the wild type (Fig. 1B), and determined the resulting exonuclease activity. No exonuclease activity was detectable in Exo5-D270A, while that of Exo5-D320A was less than 10^{-4} times that of the wild type (Fig. 2C). This analysis not only confirms that *EXO5* actually encodes the exonuclease but also lends strength to the threading analysis indicating that Exo5 belongs to the RecB family of nucleases.

Exo5 is a single-strand-specific 5′ exonuclease. Previous enzymatic studies with a partially purified preparation of Exo5 showed that the enzyme is specific for ssDNA and releases primarily dinucleotides as products. (3). We carried out a more thorough investigation of the enzymatic properties of the pure enzyme. First, we tested whether Exo5 has endonuclease activity. A 34-mer linear oligonucleotide was circularized, and activity on the circular substrate was compared with that of the linear substrate. No activity was detected on the circular oligonucleotide (Fig. 3A). We repeated this experiment with a 3-kb-long ssDNA circular plasmid. Again, no degradation by Exo5 was detected unless the circle was first linearized with a restriction endonuclease (Fig. 3B). From these experiments, we conclude that any possible endonuclease activity by Exo5 should be at least 10^5-fold lower, on a nucleotide basis, than the exonuclease activity.

Next, we labeled a 20-mer oligonucleotide either at the 5′ end with T4 polynucleotide kinase or at the 3′ end by extension with terminal transferase of a single [^{32}P]dAMP residue (see Materials and Methods). Exo5 was incubated with a 10-fold molar excess of DNA substrate, and digestion was followed over time. Digestion of the 5′-^{32}P-labeled oligonucleotide with Exo5 yielded mainly the dinucleotide as a product, while longer products, 4 to 7 nt in length, made up a total of ~5% of the digestion products (Fig. 4A, lanes 3 to 6). These longer products disappeared at longer incubation times. On the other hand, incubation of the 3′-^{32}P-labeled oligonucleotide under the exact same conditions generated a ladder of intermediates of odd lengths, consistent with a model in which the enzyme sequentially releases dinucleotides from the 5′ terminus of the 21-mer oligonucleotide (Fig. 4B, lanes 4 to 7). The starting 21-mer oligonucleotide was contaminated with ~10% 22-mer due to the addition of two dAMP residues during labeling (Fig. 4B, lane 3). This contamination likely accounted for the presence of small amounts of even-sized oligonucleotides in the digest. These data strongly indicate that Exo5 is a 5′ exonuclease and releases dinucleotides as main products of catalysis.

Exo5 showed no detectable nuclease activity when the 5′ ^{32}P oligonucleotide was completely double stranded (Fig. 4A, lane 12). Activity at the 5′-^{32}P-labeled end was not affected when just the 3′ end was made double stranded by hybridization of a 14-mer, leaving 6 nt single stranded at the 5′ end (Fig. 4A, lanes 7 to 10). However, no dinucleotide was produced when only the 5′ end was made double stranded (Fig. 4A, lane 11). Interestingly, a 16-mer product was made at an ~50-fold-reduced rate compared to the single-stranded control. This 16-mer could not have resulted from endonucleolytic activity since Exo5 has none (Fig. 3). However, generation of the 16-mer product could have resulted from 3′ loading of Exo5 with low efficiency, followed by cutting 4 nt in from the terminus or, alternatively, Exo5 could have loaded at the double-stranded end at a reduced rate and, after sliding across the double-stranded DNA (dsDNA) region, cut 2 nt downstream from the dsDNA-ssDNA junction. Based upon studies with the

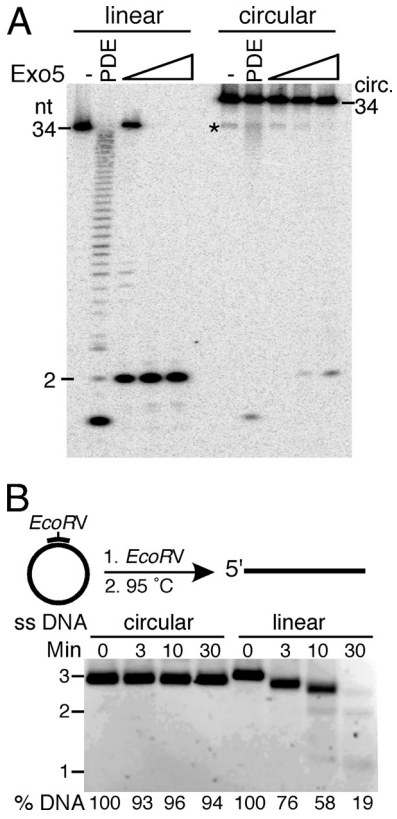

FIG. 3. Exo5 lacks endonuclease activity. (A) Standard nuclease assay mixtures contained either 10 nM linear or circular 34-mer oligonucleotide ^{32}P-c81 (see Materials and Methods) and 1 nM, 10 nM, or 100 nM Exo5. Analysis was on a 7 M urea–20% polyacrylamide gel. Note that the circular (circ.) oligonucleotide migrates slower than the linear form and is contaminated with 5% linear form (asterisk). This contaminating linear form is converted into the dinucleotide by Exo5. PDE, snake venom phosphodiesterase ladder. (B) Standard assay mixtures contained 5 nM circular or linear bluescript SK2 ssDNA (linearized by hybridizing a 12-mer oligonucleotide across the EcoRV site, followed by cutting with EcoRV and heating to restore complete single strandedness) and 200 nM Exo5. Aliquots taken after the indicated times were analyzed on a 1.2% agarose gel. Note that under these conditions the linear form migrates slightly slower that the circular form.

3′-labeled substrate discussed below, we conclude that the latter model is most likely.

Next, we assayed enzymatic activity on 3′-end-labeled substrates. No nuclease activity was detected on the fully double-stranded substrate (Fig. 4B, lane 13). When only the 3′ end was made double stranded, the primary product was 17 nt in length and was followed by a 15-mer at a reduced rate. This again indicates that Exo5 digests from the 5′ end but cuts with limited efficiency at the dsDNA-ssDNA junction (Fig. 4B, lanes 8 to 11). When just the 5′ end was made double stranded, di- and trinucleotides were produced, similar to the results observed with the single-stranded oligonucleotide, but they were produced at an ~50-fold reduced rate (Fig. 4B, lane 12). Together with the data from the 5′-labeled substrate, these data are most consistent with the ability of Exo5 to load at dsDNA ends with low efficiency and slide across dsDNA, followed by initiation of degradation at a position 2 nt down from the dsDNA-ssDNA junction.

To determine Exo5 activity at or close to junctions, we carried out a comprehensive analysis with different partially double-stranded substrates (summarized in Table 1). A partially dsDNA substrate with a 4-nt 5′ overhang is cut as efficiently as ssDNA (compare entry 5 with entry 1); however, a 2-nt 5′ overhang shows only 2.8% activity and a single-nucleotide overhang is inactive (entries 4 and 3). Exo5 also cuts pseudoforks with a similar substrate preference, showing full activity as long as 4 nt of the 5′ strand are single stranded (entry 7). As expected from the substrate specificity displayed by the enzyme, model Holiday junctions were not cut by Exo5 (data not shown).

Exo5 slides across RNA regions to engage downstream DNA. Incubation of Exo5 with labeled RNA yielded little or no digestion products, indicating that the enzyme shows sugar specificity (data not shown). However, how does the enzyme react with chimeric RNA-DNA molecules such as those that might arise as a result of RNA-primed DNA synthesis? Exo5 was incubated with oligonucleotides with increasing-length sections of 5′ RNA (Fig. 5A). Remarkably, while incubation with pT_{12} released the dinucleotide pTpT, incubation with pUT_{11}, pU_2T_{10}, and pU_3T_9, yielded tri-, tetra-, and pentanucleotides, respectively, indicating that the enzyme cuts selectively 2 nt downstream of the RNA-DNA junction. Since we know from the analyses described above that Exo5 shows neither endonuclease activity nor 3′ exonuclease activity, we conclude that Exo5 binds to 5′ RNA termini and, after sliding across the RNA substrate, cuts the DNA 2 nt from the RNA-DNA junction. The rates of hydrolysis do not decrease significantly with the addition of increasing 5′ RNA sections, indicating that loading of Exo5 at the 5′ terminus and sliding across RNA do not constitute a rate-limiting step in the reaction. This type of analysis was repeated with a chimeric oligonucleotide containing 10 ribonucleotides, followed by 11 deoxyribonucleotides, and in addition a 5′ biotin label that allows blocking of the 5′ end by streptavidin binding (Fig. 5B). With the unblocked $RNA_{10}DNA_{11}$ oligonucleotide, the major cut site was at position 12, 2 nt downstream of the RNA-DNA junction, and the rate of cutting was reduced to about 50% of that of the comparable DNA oligonucleotide (compare lanes 8 and 9 with lanes 2 and 3). However, when the 5′ end was blocked with a biotin-streptavidin moiety, only residual nuclease activity was observed, indicating that Exo5 has to load at the 5′ RNA end and slide across the RNA prior to cutting downstream DNA (lanes 14 and 15). As demonstrated above, converting the oligonucleotides to a double-stranded state abrogated all nuclease activity (lanes 4 and 5, lanes 10 and 11, and lanes 16 and 17). This specificity suggests that if Exo5 were involved in the processing of RNA-primed DNA replication intermediates, it would require prior strand displacement synthesis by the DNA polymerase or the participation of a 3′-5′ helicase, e.g., Hmi1, in order to generate the appropriate substrate for digestion (30).

Mitochondrial defects of *EXO5* mutants. The large-scale gene deletion project already indicated that *EXO5* (*DEM1*) deletions are respiration deficient (12). To confirm this mitochondrial phenotype, we made a *his3*Δ/*his3*Δ diploid strain heterozygous for *EXO5*/*exo5*Δ::*HIS3*. After sporulation, tet-

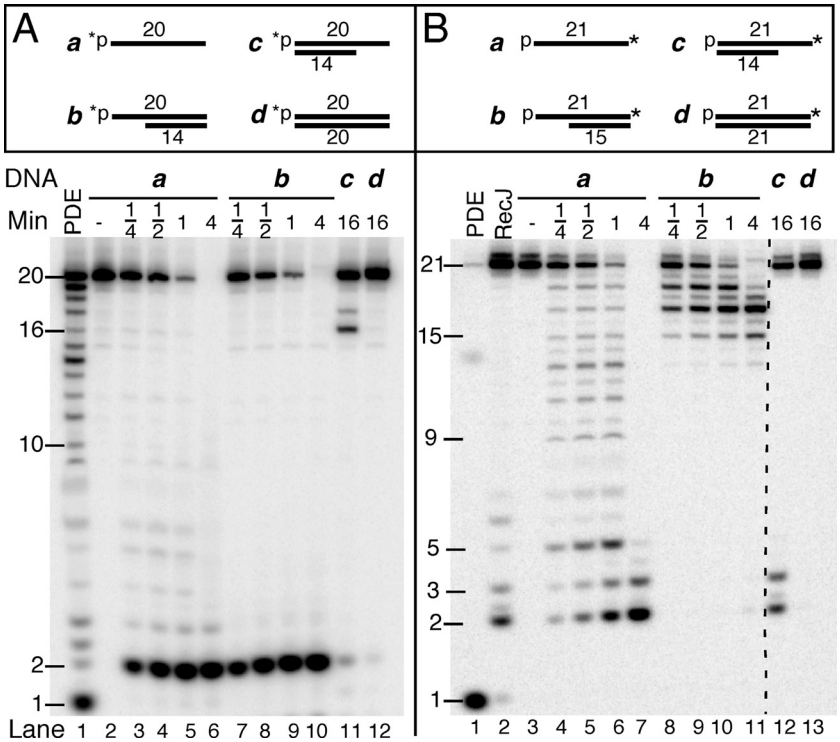

FIG. 4. Substrate specificity of Exo5. (A) 5′-labeled substrates. 5′-^{32}P-labeled v31 was either single stranded (a) or hybridized to a twofold excess of oligonucleotide c50 (b), oligonucleotide c49 (c), or oligonucleotide c41 (d). (B) 3′-labeled substrates. 3′-P-v31-^{32}P-dA was either single stranded (a) or hybridized to a twofold excess of oligonucleotide cT50 (b), oligonucleotide c49 (c), or oligonucleotide cT41 (d). An asterisk indicates the position of the label. All of the assay mixtures contained 10 nM labeled substrate, 200 mM NaCl, and 10 nM Exo5 for the indicated times at 30°C. Assay mixtures were analyzed on 7 M urea–20% polyacrylamide gels. PDE, partial digestion with snake venom phosphodiesterase, a 3′ exonuclease; RecJ, partial digestion with *E. coli* RecJ, a 5′ exonuclease. A dotted guide line is added in panel B. The values on the left of each panel are oligomer sizes.

TABLE 1. DNA substrate specificity for Exo5[a]

Expt	DNA	Sequence	% Activity
1	v31	5′-GCCCAT----	100
2	c41	3′-CGGGTA----	<0.01
	v31	5′-GCCCAT----	
3	c42	3′-GGGTA----	0.05
	v31	5′-GCCCAT----	
4	c43	3′-GGTA----	2.6
	v31	5′-GCCCAT----	
5	c44	3′-TA----	78
	v31	5′-GCCCAT----	
6	c45	3′-T_{10}CGGGTA----	<0.01
	v31	5′-GCCCAT----	
7	c48	3′-T_{10}TA----	113
	v31	5′-GCCCAT----	

[a] Standard assay mixtures contained 100 fmol single-stranded 5′-labeled oligonucleotide v31 (experiment 1) or 100 fmol 5′-labeled oligonucleotide v31 hybridized to 200 fmol of the indicated oligonucleotide and either 10, 100, or 1,000 fmol of Exo5 for 1, 3, or 10 min (see Materials and Methods). One hundred percent activity corresponds to 0.14 dinucleotide released per second per Exo5 molecule.

rads were dissected onto YPD plates. A 2:2 segregation was observed for histidine prototrophy, and all His^+ colonies failed to grow on YPG plates, i.e., containing 5% glycerol as a nonfermentable carbon source, while all His^- colonies did grow on YPG (data not shown). The tetrad analysis was repeated, but this time spores were directly germinated onto YPG plates. Each of the 14 tetrads dissected yielded a maximum of two colonies that were all His^-. Therefore, even under selective conditions, cells lacking *EXO5* are respiration deficient.

In order to determine whether the nuclease activity of Exo5 was required to maintain respiration proficiency, we first made strain PY209, which is *exo5*Δ::*HIS3* but is wild type ([*rho*$^+$]) because of the presence of a complementing *EXO5* plasmid with a *URA3* selectable marker. We then transformed this strain with a *TRP1* plasmid with wild-type *EXO5*, *exo5-D270A*, *exo5-D320A*, or the empty vector and asked whether the *URA3* plasmid could be evicted by growth on 5-fluoroorotic acid (FOA) media, either on plates containing glucose or on plates containing glycerol. While all four strains produced colonies on FOA-glucose plates, only the strain with wild-type *EXO5* produced colonies on FOA-glycerol plates (Fig. 2D). This analysis shows that the nuclease activity of Exo5 is essential for respiration proficiency and therefore indicates an essential role for Exo5 exonuclease activity in the maintenance of the mitochondrial genome.

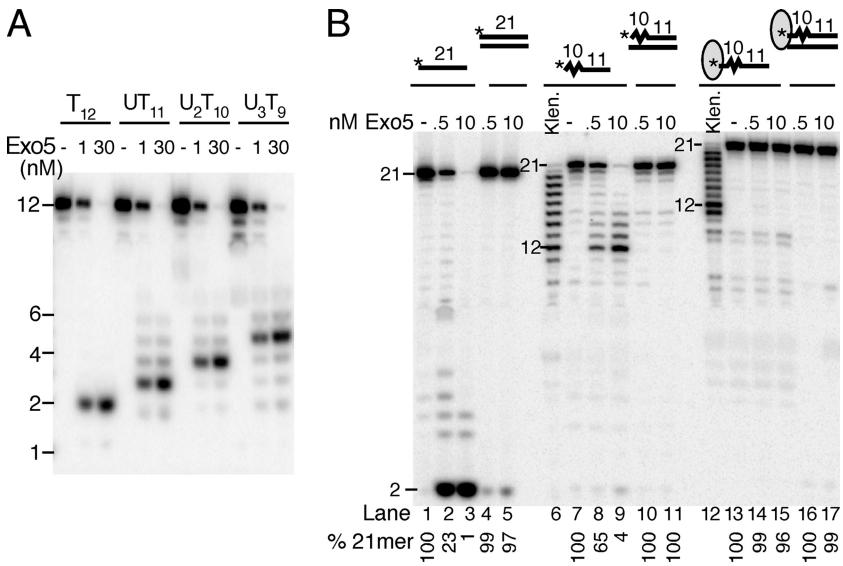

FIG. 5. Exo5 slides across 5′ RNA sequences. (A) Standard assay mixtures contained the indicated 5′-labeled DNA or RNA-DNA chimera at 10 nM/either 1 or 30 nM Exo5 for 5 min at 30°C. Assay mixtures were analyzed on a 7 M urea–20% polyacrylamide gel. (B) Standard assay mixtures contained the indicated 5′-labeled DNA or RNA-DNA chimera at 10 nM (in order from the left) v71, v71/c72, vR73, vR73/c72, Bio-vR74 plus streptavidin, or Bio-vR74/c72, plus streptavidin. Assay mixtures contained either 0.5 or 10 nM Exo5 for 5 min at 30°C and were analyzed on 7 M urea–20% polyacrylamide gels. Klen., sequence ladder generated by partial degradation with the DNA polymerase I Klenow fragment. The values beside the lanes are oligomer sizes.

Analysis of petite phenotypes in *exo5*Δ yeast. Yeast strains can become petite because of rearrangement or partial deletions of the mitochondrial genome ([*rho*$^-$]) or because of the deletion of all mitochondrial DNA ([*rho*^{0}]). The latter phenotype is, for example, observed in *mip1*Δ mutant strains defective for the mitochondrial DNA polymerase. In petites that arise from gross deletions in the genome ([*rho*$^-$]), the DNA region retained is rapidly amplified, resulting in a total mitochondrial DNA content similar to that of the wild type (reviewed in reference 1). Many [*rho*$^-$] mutants retain a short, tandemly repeated conserved segment of ~250 bp called the ORI sequence. The wild-type genome contains eight ORI sequences that are located throughout the genome. They show a high degree of sequence identity (~80%), and the A/T-rich cores of all ORI sequences are bordered by identical G/C-rich sequences. ORI sequences are found as amplified repeats in [*rho*$^-$] strains of yeast (15, 22).

We generated petites by eviction of a complementing *EXO5* plasmid from an *exo5*Δ mutant strain. The colonies arising from 11 independent events were picked and grown on YPD for 30 generations by serial dilution. Total DNA was prepared, and the mitochondrial genome was examined by PCR with sets of primers that map to different regions of the mitochondrial genome. Control strains were wild type ([*rho*$^+$]) and *mip1*Δ mutant ([*rho*^{0}]). The primer sets map to the *AI1* gene (coordinates 16.3 to 17.4 kb on the 86-kb circular mitochondrial genome) or to the *COX2* gene (coordinates 73.8 to 75.2 kb). We also used a primer set (ori-in) that amplifies the various mitochondrial ORI sequences because of their identical G/C-rich border sequences (30). In the wild-type strain, PCR products were observed with all three primer sets while PCR of total DNA isolated from the *mip1*Δ mutant strain showed no detectable PCR product with any of the primer sets. Ten out of 11 petite isolates yielded an abundant PCR product with the ori-in primer set, compared to the wild type. However, none gave a PCR product with the *AI1* primer set or the *COX2* primer set (data not shown). We conclude that loss of Exo5 nuclease leads to deletion of major genomic regions and amplification of the ORI region(s). The petite isolates were grown further for a cumulative 90 generations, and the total DNA was analyzed again. Two out of the 11 isolates now failed to produce a PCR product with the ori-in primers, suggesting a complete loss of mitochondrial DNA in these two isolates (Fig. 6B). Sequence analysis of the ~250-nt PCR products of the nine remaining clones showed that each isolate contained one single ORI sequence, either *ori3* (coordinates 54.6 to 54.8 kb; three isolates) or *ori5* (coordinates 82.3 to 82.6 kb; six isolates).

Amplification of a particular ORI sequence in petites generally produces head-to-tail repeats of the ORI sequence with variable neighboring DNA. These neighboring sequences should be identifiable by PCR analysis with a primer set complementary to the ori-in primers (ori-out, Fig. 6A). Indeed, PCR with the ori-out primers showed prominent products for each isolate, confirming that the generation of petites had occurred through head-to-tail amplification of an ORI sequence-containing region. Remarkably, the ori-out PCR consistently identified products with a very distributive size distribution (Fig. 6B). This diffuse distribution could result either from a variability in the repeat lengths generated during establishment of the petite genome or from a general genomic instability in the *exo5*Δ petite cells during continued growth (Fig. 6B). A Southern blot analysis was carried out with total mitochondrial DNA isolated from these clones and digested with restriction endonuclease EcoRV by using *ori3* and *ori5* DNAs as hybridization probes. This analysis confirmed the pattern of strong mitochondrial repeat length variability (Fig. 6C). Some isolates also showed a

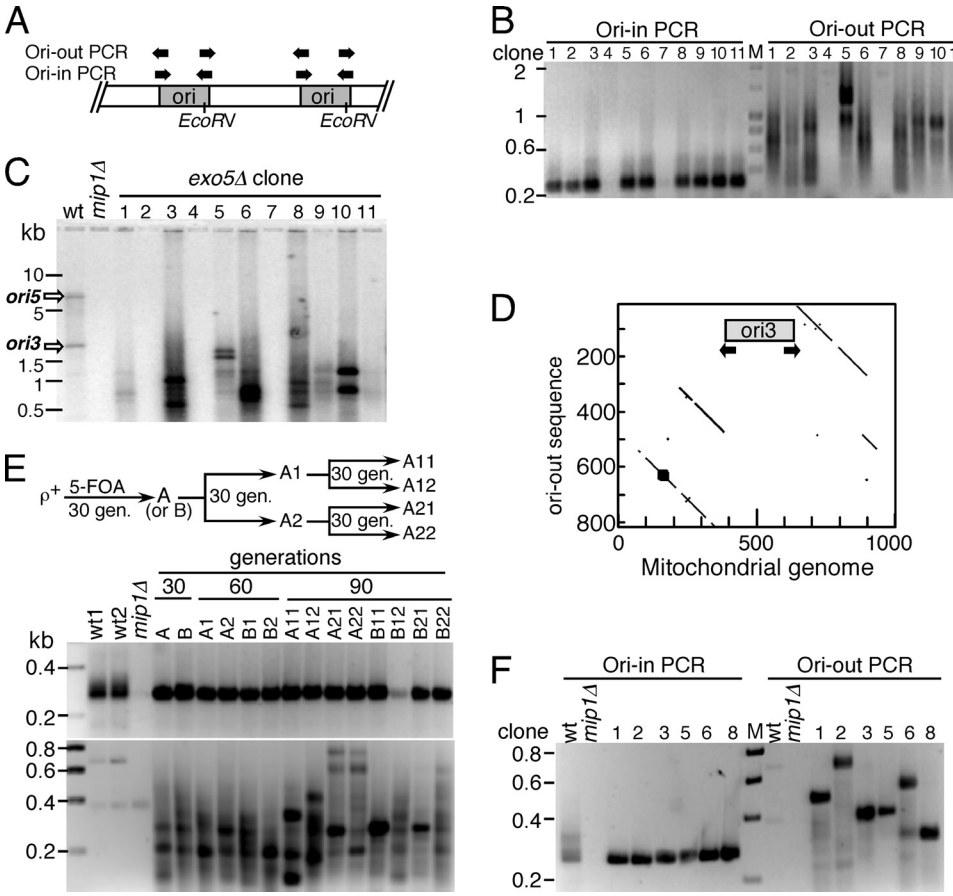

FIG. 6. Analysis of mitochondrial DNA in *exo5*Δ petite mutants. (A) Head-to-tail arrangement of amplified ORI regions. A unique EcoRV restriction site localized asymmetrically in both *ori3* and *ori5* is shown. The ori-in and ori-out primers were used for PCR analysis of either the ORI sequences or the inter-ORI sequence regions, respectively. (B) PCR analysis of DNA from 11 individual *exo5*Δ clones after 90 generations of growth. (C) Southern analysis of total yeast DNA from the clones in panel B, digested with EcoRV, and probed with a mixture of *ori3* and *ori5* probes. The probes were generated by PCR labeling of mitochondrial DNA obtained from *ori3*- and *ori5*-containing petites. Analysis of DNA from the wild type (lane 1) shows the expected sizes for the wild-type (wt) *ori3* and *ori5* EcoRV fragments, marked with arrows. (D) The ori-out PCR products shown in panel B were sequenced in both directions. The presence of different overlapping sequence runs allowed only approximate sequence determination. For one representative clone, a matrix analysis of the ori-out sequence with that of the mitochondrial genome is shown (coordinates 54168 to 55167), identifying a 23-nt identity per 25-nt sliding window. Regions directly to the left and right of *ori3* were identified; two internal repeats are apparent. (E) Instability of [*rho*$^-$] genomes during serial propagation. Two independent clones (clone A with *ori3* amplified and clone B with *ori5* amplified) were obtained by eviction of *EXO5* from PY209 and grown for 30 generations (gen.) by serial dilution. They were plated on YPD, and two colonies were picked (A1 and A2 for the experiment with clone A) and grown for another 30 generations. Again, two colonies were picked per culture, yielding clones A11, A12, A21, and A22, and grown. The scheme for clone A is shown; the clone B scheme was the same. DNA from each isolate was prepared and subjected to PCR analysis with ori-in primers (top) and ori-out primers (bottom). (F) Clones 1, 2, 3, 5, 6, and 8 (as shown in panel B) were transformed with pBL253 (*URA3 EXO5*), and DNA from one transformant of each clone was subjected to PCR analysis.

reduction in hybridization strength, particularly isolates 2 and 11, which is presumably due to partial loss of the mitochondrial genome in subpopulations of cells. Furthermore, as expected, isolates 4 and 7, which were [*rho*^{0}], showed no hybridization signal.

We reasoned that in the absence of Exo5, each mitochondrial replication cycle might be associated with a high probability of genome rearrangements and duplications, leading to a dynamic variability in the sizes of the amp icons by PCR and by Southern analysis. We sequenced the ori-out PCR products from the nine clones shown in Fig. 6B (right panel). Overlapping sequences were identified in all of the clones, prohibiting accurate sequence assignment. However, for several isolates, a specific sequence predominated and could be mapped to regions directly to the left and right of either *ori3* or *ori5*. Importantly, this analysis showed that the sequences flanking *ori3* or *ori5* contained additional internal repeat sequences between 50 and 200 nt in length, suggesting that recombination frequently occurred in the *exo5*Δ clones (Fig. 6D). We confirmed the high-instability phenotype of *exo5*Δ mutants by carrying out an experiment in which two independently isolated *exo5*Δ clones, one with *ori3* amplified and one with *ori5* amplified, were serially propagated and expanded through successive growth cycles, and individual clones were analyzed by PCR. The two clones produced after loss of *EXO5* persistently altered their ori-out PCR patterns upon serial propagation (Fig. 6E).

We next tested whether the reintroduction of *EXO5* into the petite clones would cause stabilization of the petite genomes.

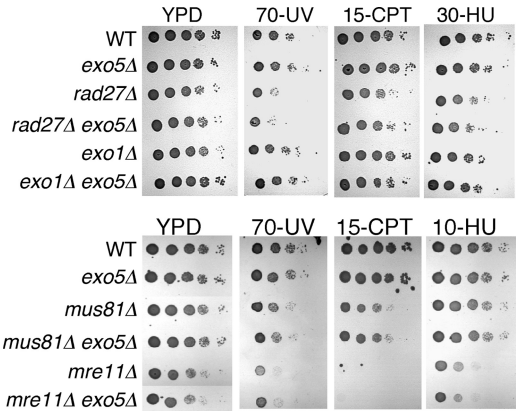

FIG. 7. *exo5*Δ mutant strains are not damage sensitive. All strains were *mip1*Δ ([*rho*^{0}]) and, in addition, had the indicated genotype. Serial 10-fold dilutions of late-log-phase cells, from 10^5 to 10 cells per spot, were spotted onto YPD plates or YPD plates containing the indicated concentrations of hydroxyurea (HU, mM) or camptothecin (CPT, μg/ml). Some YPD plates were irradiated with the indicated fluency of UV_{254}. Plates were grown for 3 days at 30°C and photographed. WT, wild type.

An *EXO5*-complementing plasmid was transformed back into randomly selected petite isolates, and the transformants were analyzed by PCR analysis with the ori-in and ori-out primers (Fig. 6F). Remarkably, the ori-out PCR product distribution had narrowed drastically, indicating that a stable repeat pattern had been established in the Exo5-containing transformants. Sequence analysis of the repeat unit identified unique wild-type sequences that border *ori3* or *ori5* on the left and right. The junction between the upstream and downstream ORI sequences varied from clone to clone. However, invariably, this junction was formed by a sequence 7 to 13 nt in length that was present in both the upstream and downstream mitochondrial genomic sequences. This observation strongly suggests that junction formation had occurred through recombination between these small identical sequence motifs.

Petite mutants can exhibit zygotic suppressiveness, a phenomenon in which, upon mating with a wild-type [*rho*$^+$] strain, the wild-type mitochondrial genome is excluded from diploids; i.e., the diploids are also [*rho*$^-$] (13). Hypersuppressiveness is a consequence of the large number of ORI sequence repeats in the [*rho*$^-$] strain. Both RNA-primed replication and recombination mechanisms contribute to hypersuppressivity (22, 24). The *exo5*Δ clones lacking mitochondrial DNA (clones 4 and 7 in Fig. 6B) showed no hypersuppressiveness upon mating with a [*rho*$^+$] strain; i.e., all diploids were wild type [*rho*$^+$]. In contrast, the other clones showed high degrees of hypersuppressiveness, from 80% to 100%; i.e., up to 100% of the diploids were [*rho*$^-$], in agreement with similar findings by others (22, 24).

***EXO5* deletion shows no nuclear phenotypes.** We explored the possibility that Exo5 may also reside in the yeast nucleus at low levels, even though it was only detected in the mitochondria (18). However, our genetic analysis identifying a potential nuclear function for Exo5 was uniformly negative. To eliminate phenotypes due to mitochondrial dysfunction, we carried out all of our studies in a [*rho*^{0}] *mip1*Δ mutant background. We compared the growth and DNA damage survival of *exo5*Δ *mip1*Δ double mutants with *mip1*Δ mutants as a control. In addition, we combined these mutants with deletions of the additional nuclease genes *RAD27*, *EXO1*, *MUS81*, and *MRE11*. The damage sensitivities of the triple mutants were compared with those of the relevant double mutants (Fig. 7). FEN1, encoded by *RAD27*, is primarily involved in Okazaki fragment maturation and base excision repair, Exo1 is involved in mismatch repair and double-strand break repair, Mus81 is involved in the processing of stalled replication forks, and Mre11 is involved in double-strand break repair (reviewed in references 2, 6, and 34). Serial dilutions were plated on YPD plates containing hydroxyurea or camptothecin, or plates were UV irradiated. No significant differences in damage sensitivity were observed between a given *mip1*Δ *nuclease* double mutant and the *exo5*Δ *mip1*Δ *nuclease* triple mutant. Therefore, we conclude that either *EXO5* is not involved in nuclear DNA maintenance or a very efficient redundancy with other nucleases exists in the DNA damage repair pathways tested.

DISCUSSION

Exo5 has the remarkable ability to slide over RNA and less efficiently over dsDNA to initiate cutting at a position 2 nt downstream of the RNA-DNA or dsDNA-ssDNA junction. The ability to differentiate between RNA and DNA but cut ssDNA flaps efficiently through sliding may be important for the maturation of intermediates during mitochondrial DNA replication. Since Exo5 does not degrade dsDNA or dsRNA-DNA, the generation of such single-stranded flaps would have to be accomplished either through strand displacement synthesis by the mitochondrial DNA polymerase γ or through the participation of a 3′-5′ helicase. The first is an important Okazaki maturation mechanism in the nucleus, where substrates for cutting by FEN1 and by Dna2 are generated through strand displacement synthesis by polymerase δ (reviewed in reference 2). Alternatively, the single-stranded flap could be generated through helicase action. The Hmi1 helicase has the correct directionality (3′-5′) to generate substrates for Exo5, and it is also essential for maintenance of the wild-type mitochondrial genome but not for that of [*rho*$^-$] petites (21, 26). Unfortunately, very little is known about the mechanism of replication of the yeast mitochondrial genome. Replication may occur through several mechanisms, including initiation by RNA polymerase and by double-strand break-induced recombinational mechanisms that can mature into rolling-circle replication (22, 28, 35). Sufficient replicative ability must remain in an *exo5*Δ mutant strain to allow replication of the ORI repeat sequences, since these cells are [*rho*$^-$] and not [*rho*^{0}]. However, the observations that 2 out of the 11 petite isolates studied lost their mitochondrial DNA and 2 more were severely depleted for mitochondrial DNA indicate that even maintenance of the [*rho*$^-$] genome is severely compromised (Fig. 6B and C).

An alternative function for Exo5 could be in recombination. We think this is unlikely because of the extreme repeat variability displayed in the *exo5*Δ mutant strains that can only be a consequence of very active recombination. All of the [*rho*$^-$] clones that we generated by eviction of *EXO5* had amplified either *ori3* or *ori5*, together with variable-length sequences surrounding either ORI sequence. These regions showed high variability during propagation, indicative of very active

recombination (Fig. 6B, C, and E). In addition, sequences inside the repeat unit were subject to additional partial duplication events, suggesting a hyperrecombination phenotype in the mutants (Fig. 6D).

The generation of conditional mutations in *EXO5* should be of invaluable help in delineating its contribution to mitochondrial genome maintenance. As Exo5 is conserved in other organisms, including humans (Fig. 2A), resolving the mechanism of yeast *EXO5* may have important implications for understanding genome stability in higher organisms.

ACKNOWLEDGMENTS

We thank David Phillips for help with the tetrad analysis, Francoise Foury for advice and strains, and John Majors for critical discussion during the progress of this study.

This work was supported in part by grant GM032431 from the National Institutes of Health.

REFERENCES

1. **Bernardi, G.** 2005. Lessons from a small, dispensable genome: the mitochondrial genome of yeast. Gene **354:**189–200.
2. **Burgers, P. M.** 2009. Polymerase dynamics at the eukaryotic DNA replication fork. J. Biol. Chem. **284:**4041–4045.
3. **Burgers, P. M. J., G. A. Bauer, and L. Tam.** 1988. Exonuclease V from Saccharomyces cerevisiae. A 5′-3′-deoxyribonuclease that produces dinucleotides in a sequential fashion. J. Biol. Chem. **263:**8099–8105.
4. **Büttner, S., T. Eisenberg, D. Carmona-Gutierrez, D. Ruli, H. Knauer, C. Ruckenstuhl, C. Sigrist, S. Wissing, M. Kollroser, K. U. Frohlich, S. Sigrist, and F. Madeo.** 2007. Endonuclease G regulates budding yeast life and death. Mol. Cell **25:**233–246.
5. **Bylund, G. O., J. Majka, and P. M. Burgers.** 2006. Overproduction and purification of RFC-related clamp loaders and PCNA-related clamps from *Saccharomyces cerevisiae*. Methods Enzymol. **409:**1–11.
6. **Ciccia, A., N. McDonald, and S. C. West.** 2008. Structural and functional relationships of the XPF/MUS81 family of proteins. Annu. Rev. Biochem. **77:**259–287.
7. **Cooper, D. L., R. S. Lahue, and P. Modrich.** 1993. Methyl-directed mismatch repair is bidirectional. J. Biol. Chem. **268:**11823–11829.
8. **de Zamaroczy, M., G. Faugeron-Fonty, G. Baldacci, R. Goursot, and G. Bernardi.** 1984. The ori sequences of the mitochondrial genome of a wild-type yeast strain: number, location, orientation and structure. Gene **32:**439–457.
9. **de Zamaroczy, M., R. Marotta, G. Faugeron-Fonty, R. Goursot, M. Mangin, G. Baldacci, and G. Bernardi.** 1981. The origins of replication of the yeast mitochondrial genome and the phenomenon of suppressivity. Nature **292:**75–78.
10. **Dimmer, K. S., S. Fritz, F. Fuchs, M. Messerschmitt, N. Weinbach, W. Neupert, and B. Westermann.** 2002. Genetic basis of mitochondrial function and morphology in Saccharomyces cerevisiae. Mol. Biol. Cell **13:**847–853.
11. **Duxin, J. P., B. Dao, P. Martinsson, N. Rajala, L. Guittat, J. L. Campbell, J. N. Spelbrink, and S. A. Stewart.** 2009. Human Dna2 is a nuclear and mitochondrial DNA maintenance protein. Mol. Cell. Biol. **29:**4274–4282.
12. **Entian, K. D., T. Schuster, J. H. Hegemann, D. Becher, H. Feldmann, U. Guldener, R. Gotz, M. Hansen, C. P. Hollenberg, G. Jansen, W. Kramer, S. Klein, P. Kotter, J. Kricke, H. Launhardt, G. Mannhaupt, A. Maierl, P. Meyer, W. Mewes, T. Munder, R. K. Niedenthal, M. Ramezani Rad, A. Rohmer, A. Romer, A. Hinnen, et al.** 1999. Functional analysis of 150 deletion mutants in Saccharomyces cerevisiae by a systematic approach. Mol. Gen. Genet. **262:**683–702.
13. **Ephrussi, B., H. de Margerie-Hottinguer, and H. Roman.** 1955. Suppressiveness: a new factor in the genetic determinism of the synthesis of respiratory enzymes in yeast. Proc. Natl. Acad. Sci. U. S. A. **41:**1065–1071.
14. **Foury, F.** 1989. Cloning and sequencing of the nuclear gene MIP1 encoding the catalytic subunit of the yeast mitochondrial DNA polymerase. J. Biol. Chem. **264:**20552–20560.
15. **Foury, F., T. Roganti, N. Lecrenier, and B. Purnelle.** 1998. The complete sequence of the mitochondrial genome of Saccharomyces cerevisiae. FEBS Lett. **440:**325–331.
16. **Graves, T., M. Dante, L. Eisenhour, and T. W. Christianson.** 1998. Precise mapping and characterization of the RNA primers of DNA replication for a yeast hypersuppressive petite by in vitro capping with guanylyltransferase. Nucleic Acids Res. **26:**1309–1316.
17. **Hoffman, C. S., and F. Winston.** 1987. A ten-minute DNA preparation from yeast efficiently releases autonomous plasmids for transformation of Escherichia coli. Gene **57:**267–272.
18. **Huh, W. K., J. V. Falvo, L. C. Gerke, A. S. Carroll, R. W. Howson, J. S. Weissman, and E. K. O'Shea.** 2003. Global analysis of protein localization in budding yeast. Nature **425:**686–691.
19. **Kalifa, L., G. Beutner, N. Phadnis, S. S. Sheu, and E. A. Sia.** 2009. Evidence for a role of FEN1 in maintaining mitochondrial DNA integrity. DNA Repair (Amsterdam) **8:**1242–1249.
20. **Koprowski, P., M. U. Fikus, P. Dzierzbicki, P. Mieczkowski, J. Lazowska, and Z. Ciesla.** 2003. Enhanced expression of the DNA damage-inducible gene DIN7 results in increased mutagenesis of mitochondrial DNA in Saccharomyces cerevisiae. Mol. Genet. Genomics **269:**632–639.
21. **Kuusk, S., T. Sedman, P. Joers, and J. Sedman.** 2005. Hmi1p from Saccharomyces cerevisiae mitochondria is a structure-specific DNA helicase. J. Biol. Chem. **280:**24322–24329.
22. **Ling, F., A. Hori, and T. Shibata.** 2007. DNA recombination-initiation plays a role in the extremely biased inheritance of yeast [*rho*$^-$] mitochondrial DNA that contains the replication origin *ori5*. Mol. Cell. Biol. **27:**1133–1145.
23. **Liu, P., L. Qian, J. S. Sung, N. C. de Souza-Pinto, L. Zheng, D. F. Bogenhagen, V. A. Bohr, D. M. Wilson III, B. Shen, and B. Demple.** 2008. Removal of oxidative DNA damage via FEN1-dependent long-patch base excision repair in human cell mitochondria. Mol. Cell. Biol. **28:**4975–4987.
24. **MacAlpine, D. M., J. Kolesar, K. Okamoto, R. A. Butow, and P. S. Perlman.** 2001. Replication and preferential inheritance of hypersuppressive petite mitochondrial DNA. EMBO J. **20:**1807–1817.
25. **Mimitou, E. P., and L. S. Symington.** 2008. Sae2, Exo1 and Sgs1 collaborate in DNA double-strand break processing. Nature **455:**770–774.
26. **Monroe, D. S., Jr., A. K. Leitzel, H. L. Klein, and S. W. Matson.** 2005. Biochemical and genetic characterization of Hmi1p, a yeast DNA helicase involved in the maintenance of mitochondrial DNA. Yeast **22:**1269–1286.
27. **Mookerjee, S. A., and E. A. Sia.** 2006. Overlapping contributions of Msh1p and putative recombination proteins Cce1p, Din7p, and Mhr1p in large-scale recombination and genome sorting events in the mitochondrial genome of Saccharomyces cerevisiae. Mutat. Res. **595:**91–106.
28. **Nosek, J., L. Tomaska, M. Bolotin-Fukuhara, and I. Miyakawa.** 2006. Mitochondrial chromosome structure: an insight from analysis of complete yeast genomes. FEMS Yeast Res. **6:**356–370.
29. **O'Rourke, T. W., N. A. Doudican, M. D. Mackereth, P. W. Doetsch, and G. S. Shadel.** 2002. Mitochondrial dysfunction due to oxidative mitochondrial DNA damage is reduced through cooperative actions of diverse proteins. Mol. Cell. Biol. **22:**4086–4093.
30. **Sedman, T., S. Kuusk, S. Kivi, and J. Sedman.** 2000. A DNA helicase required for maintenance of the functional mitochondrial genome in *Saccharomyces cerevisiae*. Mol. Cell. Biol. **20:**1816–1824.
31. **Singleton, M. R., M. S. Dillingham, M. Gaudier, S. C. Kowalczykowski, and D. B. Wigley.** 2004. Crystal structure of RecBCD enzyme reveals a machine for processing DNA breaks. Nature **432:**187–193.
32. **Söding, J.** 2005. Protein homology detection by HMM-HMM comparison. Bioinformatics **21:**951–960.
33. **Stith, C. M., J. Sterling, M. A. Resnick, D. A. Gordenin, and P. M. Burgers.** 2008. Flexibility of eukaryotic Okazaki fragment maturation through regulated strand displacement synthesis. J. Biol. Chem. **283:**34129–34140.
34. **Tran, P. T., N. Erdeniz, L. S. Symington, and R. M. Liskay.** 2004. EXO1-A multi-tasking eukaryotic nuclease. DNA Repair (Amsterdam) **3:**1549–1559.
35. **Wanrooij, S., J. M. Fuste, G. Farge, Y. Shi, C. M. Gustafsson, and M. Falkenberg.** 2008. Human mitochondrial RNA polymerase primes lagging-strand DNA synthesis in vitro. Proc. Natl. Acad. Sci. U. S. A. **105:**11122–11127.
36. **Yeeles, J. T., R. Cammack, and M. S. Dillingham.** 2009. An iron-sulfur cluster is essential for the binding of broken DNA by AddAB-type helicase-nucleases. J. Biol. Chem. **284:**7746–7755.
37. **Yu, M., J. Souaya, and D. A. Julin.** 1998. Identification of the nuclease active site in the multifunctional RecBCD enzyme by creation of a chimeric enzyme. J. Mol. Biol. **283:**797–808.
38. **Zassenhaus, H. P., T. J. Hofmann, R. Uthayashanker, R. D. Vincent, and M. Zona.** 1988. Construction of a yeast mutant lacking the mitochondrial nuclease. Nucleic Acids Res. **16:**3283–3296.
39. **Zheng, L., M. Zhou, Z. Guo, H. Lu, L. Qian, H. Dai, J. Qiu, E. Yakubovskaya, D. F. Bogenhagen, B. Demple, and B. Shen.** 2008. Human DNA2 is a mitochondrial nuclease/helicase for efficient processing of DNA replication and repair intermediates. Mol. Cell **32:**325–336.